JPNT 8(2), 41-47 (2019)
https://doi.org/10.11003/JPNT.2019.8.2.41

JPNT Journal of Positioning, Navigation, and Timing

# A Model to Evaluate Jammer Influences on Ranging Measurements

Won Jae Yoo[1], Heyone Kim[2], Dong-Hwan Hwang[2], Hyoungmin So[3], Hyung Keun Lee[1†]

[1]School of Electronics and Information Engineering, Korea Aerospace University, Goyang 10540, Korea
[2]Department of Electronics Engineering, Chungnam National University, Daejeon 34134, Korea
[3]Agency for Defense Development, Daejeon 34186, Korea

## ABSTRACT

Recently, number of intentional jamming has increased significantly. If GNSS jammers are activated, user receivers can be largely influenced due to the vulnerable characteristic of the GNSS (Global Navigation Satellite System) signal. When the reception power of the jamming signal and that of the navigation signal are similar, the C/A (Coarse Acquisition) chip delay error can occur in the delay locked loop. To evaluate the jamming effect, a new measurement model is formulated based on previous research works. The new model explains how the jamming to signal ratio affects the ranging measurement accuracy and other parameters. To evaluate the validity of the newly formulated model, the experiment results of the previous research works under actual jamming environment are utilized. By evaluating the consistency of the carrier-to-noise ratio (C/N0) and the position error with the actual jamming environment, the validity of the newly formulated model is verified.

**Keywords:** GNSS, jamming, vulnerability, pseudorange

## 1. INTRODUCTION

The satellites located around 20,000 km higher than the ground are transmitting navigation signals to the earth in Global Navigation Satellite Systems (GNSSs), which are operated by the U.S., Russia, EU, and China. The received signal power on the ground is very weak as -160 dBW. Thus, signals are highly sensitive to intentional jamming or surrounding environments (Grant et al. 2009).

A jamming technique refers to the transmission of intentional strong disturbance signals to the frequency band used in navigation signals thereby preventing users from receiving navigation signals. Thus, if an intentional jamming occurs, ranging measurements cannot be received normally, thereby making the calculation of user's navigation solution difficult. In addition, navigation signals cannot be tracked continuously or will be lost within seconds to minutes (Choi & Ko 2015).

The jamming technique applied to GNSS signals can be divided into the wideband and narrowband types. The wideband jamming refers to the technique that wideband-modulated signals put jamming effects over the frequency band of navigation signals. This technique consumes large power and cost. In contrast, the narrowband jamming is the technique that narrowband-modulated signals put a jamming effect in a specific GNSS frequency band, which is easy to produce by using a small-size jammer. For wideband jamming, studies have been conducted mainly on imposing hostile Gaussian noise over GNSS frequency bands. On the other hand, for narrowband jamming, there have been several different studies: tone jamming type of continuous wave, sweep jamming type with varying frequency, pulse jamming type that is effective to a direct sequence spread spectrum system, and harmonic frequency jamming type (Kim 2013).

**Received** Feb 25, 2019 **Revised** May 01, 2019 **Accepted** May 03, 2019
†**Corresponding Author**
E-mail: hyknlee@kau.kr
Tel: +82-2-300-0131 Fax: +82-2-3158-5769
**Won Jae Yoo** https://orcid.org/0000-0002-6683-2120
**Heyone Kim** https://orcid.org/0000-0002-4291-3030
**Dong-Hwan Hwang** https://orcid.org/0000-0002-0933-5881
**Hyoungmin So** https://orcid.org/0000-0001-5279-8833
**Hyung Keun Lee** https://orcid.org/0000-0001-5210-1557

**Table 1.** Comparison of ranging measurement influence by jamming signal power.

| Case | Signal strength | Result |
|---|---|---|
| Case 1 | Jamming signal ≪ Navigation signal | Normal operation (Receive the normal navigation signal) |
| Case 2 | Jamming signal ≥ Navigation signal | Obtain the navigation signal (Include ranging measurement error) |
| Case 3 | Jamming signal ≫ Navigation signal | Navigation signal unable (Cannot receive the navigation signal) |

In addition, various anti-jamming techniques have been studied to effectively cope with jamming attacks in a navigation warfare environment. For example, studies on beam steered array technique that increases the gain by forming a very narrow beam width and controlled reception pattern that forms a null to the jammer direction have been conducted (De Lorenzo et al. 2006). Furthermore, a front-end filtering technique that blocks jamming signal using a bandwidth filter with sharp cutoff and measuring a jamming to noise ratio in automatic gain control have been studied.

A pre-processing technique that removes jamming and interference signals using digitalized signal samples before navigation signals are modulated in the receiver, a code and carrier tracking loop technique, a technique to estimate the position of multi-jammers by using multiple monitor stations, and a combined technique with inertial navigation systems and multiple navigation signals have been studied (Fu & Zhu 2011). According to the navigation signal frequency, anti-jamming techniques can be divided into two cases where the same frequency bands of existing navigation systems are used or other separate frequency bands are used.

To deal with jamming effects in more detail, this paper proposes an effective model describing jammer influence on ranging measurements. The proposed model can be applied when the jamming signal power is similar to the navigation signal power in a navigation warfare situation. It should be noted that the signal tracking loop does not work and no ranging measurement can be generated when the jamming signal power is larger than the navigation signal power. The proposed model explains how the number of visible satellites, the carrier-to-noise ratio (C/N0), and the jamming-to-signal ratio (J/S) affects ranging measurement errors. The validity of the proposed ranging error model is indirectly verified by utilizing the existing jamming experiment results reported in the previous research works.

## 2. JAMMING INFLUENCE MODEL OF RANGING MEASUREMENTS

When jamming attacks occur in navigation warfare situations, the effects on navigation measurement can be divided into three cases according to the relative power between the jamming signal and the navigation signal as presented in Table 1. Case 1 in Table 1 refers to the normally received navigation signal as no jamming effect on the user's receiver is determined. In this case, the received jamming signal intensity is weaker than that of the navigation signal. Case 2 refers to the case where the jamming power and the navigation signal power are similar. In this case, errors in ranging measurements might be enlarged as the jamming signal influences receiver operation. In general, ranging error increases in proportion to the influence level on the ranging measurement. Case 3 refers to the case where the jamming signal power is much larger than the navigation signal power. In this case, users cannot receive the navigation signal as the jamming signal overrides the navigation signal (Glomsvoll 2014).

**Table 2.** Description of parameters on signal propagation in free space.

| Parameter | Description |
|---|---|
| $(EIRP_j)_{dB}$ | Effective isotropic radiated power (EIRP) = $(J_t)_{dB} + (G_t)_{dB}$ |
| $(J_t)_{dB}$ | Jammer transmission power (dBW) = $10\log_{10}(J_t)_W$ |
| $(G_t)_{dB}$ | Jammer transmission antenna gain (dBic) |
| $(J_r)_{dB}$ | Received jamming signal power (dBW) = $10\log_{10}(J_r)_W$ |
| $(L_p)_{dB}$ | Free space propagation loss (dB) = $20\log_{10}(4\pi d/\lambda_j)$ |
| $d$ | Distance between jammer and user (m) |
| $f_j$ | Jamming frequency (Hz) |
| $\lambda_j$ | Wavelength of jamming frequency (m) = $c/f_j$ |
| $c$ | Speed of light (m/sec) |
| $(G_j)_{dB}$ | Receiver antenna gain toward jammer direction (dBic) |
| $(L_f)_{dB}$ | Signal loss by receiver front-end filtering (dB) |

To calculate the level of influence on the ranging measurement, the received jamming signal power needs to be calculated. Considering the free space path loss, it can be calculated by Eq. (1) considering the distance between jammer and the receiver, the jammer's transmission power, and the jamming frequency band (Kim 2013). The variables related to Eq. (1) are summarized in Table 2.

$$\begin{aligned}(J_r)_{dB} &= (EIRP_j)_{dB} + (G_j)_{dB} - (L_p)_{dB} - (L_f)_{dB} \\ &= (J_t)_{dB} + (G_t)_{dB} + (G_j)_{dB} - (L_p)_{dB} - (L_f)_{dB} \\ &= 10\log_{10}(J_t)_W + (G_t)_{dB} + (G_j)_{dB} - 20\log_{10}\left(\frac{4\pi d}{\lambda_j}\right) - (L_f)_{dB} \end{aligned} \quad (1)$$

Based on Eq. (1), the jamming to signal ratio $(J/S)_{dB}$ in dB unit can be calculated by Eq. (2) where $(S_r)_{dB}$ denotes the received navigation signal power. Fig. 1 shows the $(J/S)_{dB}$ variation according to the distance between the jammer and the receiver with $f_j$ = 1575.42 MHz, $G_t$ = 3 dB, $G_j$ = 6 dB, and $L_f$ = 3 dB, and $S_r$ = -157.5 dB.

$$(J/S)_{dB} = (J_r)_{dB} - (S_r)_{dB} \quad (2)$$

The jamming to signal ratio computed by Eq. (2) is affected

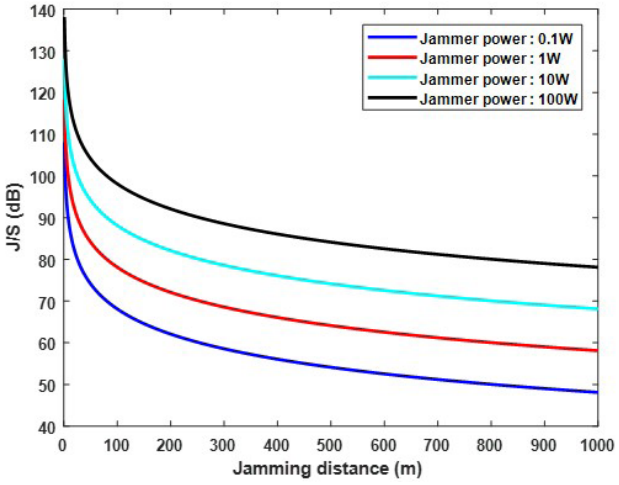


**Fig. 1.** Comparison of J/S variation with jammer power and jamming distance.

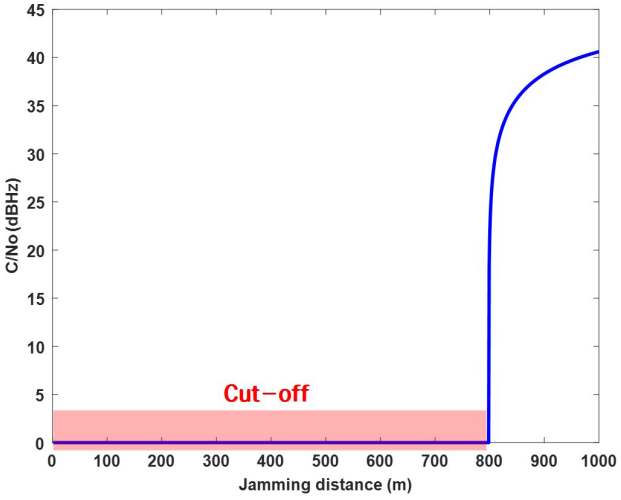


**Fig. 2.** Calculated C/N0 by jamming distance variation.

by the carrier-to-noise ratio $(C/N_0)_{dBHz}$ at the receiver, the threshold value $(C/N_0)_{eff,dBHz}$, the antenna gain towards the satellite $(G_{svi})_{dB}$, the antenna gain towards the jammer $(G_j)_{dB}$, the jamming resistance quality factor $Q$, and the code chip rate $R_c$ (Kaplan & Hegarty 2005). By re-arranging Eq. (3) with regard to $(C/N_0)_{dBHz}$, Eq. (4) can also be obtained.

$$(J/S)_{dB} = -(G_{svi})_{dB} + (G_j)_{dB} + 10\log_{10}\left[Q \cdot R_c \left(10^{-\frac{(C/N_0)_{eff,dBHz}}{10}} - 10^{-\frac{(C/N_0)_{dBHz}}{10}}\right)\right] \quad (3)$$

$$(C/N_0)_{dBHz} = -10\log_{10}\left(10^{-\frac{(C/N_0)_{eff,dBHz}}{10}} - \frac{1}{Q \cdot R_c} 10^{\frac{(J/S)_{dB}+(G_{svi})_{dB}-(G_j)_{dB}}{10}}\right) \quad (4)$$

Fig. 2 shows the change in $(C/N_0)_{dBHz}$ according to the changes in jamming distance from the receiver when $G_{svi}$ =1.5 dB, $Q$ = 2.22, $R_c$ = 1.023 Mcps, and $(C/N_0)_{eff,dBHz}$ = 28 dBHz. When $J_t$ = 0.01 W and all the other variables are the same as those used in generating Fig. 1, $(C/N_0)_{dBHz}$ can be calculated using $(J/S)_{dB}$ computed according to the change in jamming distance. As verified in Fig. 2, $(C/N_0)_{dBHz}$ cannot be calculated when the jamming distance was 800 m or shorter as $(J/S)_{dB}$ is calculated to a large value. However, $(C/N_0)_{dBHz}$ increased as the jamming distance increased when the jamming distance was 800 m or longer.

When jamming signal power is at the similar level with the navigation signal power during the normal signal tracking process of a navigation receiver, unstable signal delays can occur due to jitter type errors generated in the delay locked loop (DLL) of the receiver. Eq. (5) describes the relationship between the DLL jitter error and $(C/N_0)_{dBHz}$ (Kaplan & Hegarty 2005). Table 3 describes the variables used in Eq. (5). The jitter error is generated differently according to the correlation between the early-to-late width D of the receiver

**Table 3.** Description of parameters on calculating DLL jitter error.

| Parameter | Description |
|---|---|
| $\sigma_{tDLL}$ | 1-sigma jitter error on DLL (chip) |
| $D$ | Chip interval in Early-to-Late correlator (chip) |
| $B_n$ | Code loop noise bandwidth (Hz) |
| $B_{fe}$ | Double-sided front-end bandwidth (Hz) |
| $T$ | Predetection integration time (sec) |
| $T_c$ | Code chip width (sec/chip) |
| $b$ | Normalized bandwidth (Hz) = $B_{fe}/R_c$ |

correlator and the normalized bandwidth $b\left(=\frac{B_{fe}}{R_c}\right)$.

$$(\sigma_{tDLL})_{chip} = \begin{cases} \sqrt{\frac{B_n}{2\cdot(C/N_0)_{dBHz}} \times D \times [1+\frac{2}{T\cdot(C/N_0)_{dBHz}\cdot(2-D)}]}, & D \geq \frac{\pi \cdot R_c}{B_{fe}} \\ \sqrt{\frac{B_n}{2\cdot(C/N_0)_{dBHz}} \times (\frac{1}{B_{fe}\cdot T_c} + \frac{B_{fe}\cdot T_c}{\pi - 1} \times (D - \frac{1}{B_{fe}\cdot T_c})^2) \times [1+\frac{2}{T\cdot(C/N_0)_{dBHz}\cdot(2-D)}]}, & \frac{R_c}{B_{fe}} < D < \frac{\pi \cdot R_c}{B_{fe}} \\ \sqrt{\frac{B_n}{2\cdot(C/N_0)_{dBHz}} \times (\frac{1}{B_{fe}\cdot T_c}) \times [1+\frac{1}{T\cdot(C/N_0)_{dBHz}}]}, & D \leq \frac{R_c}{B_{fe}} \end{cases} \quad (5)$$

Since the jitter error calculated by Eq. (5) is in chip length unit, it is converted to m unit by Eq. (6) that can be interpreted as the ranging measurement error. Fig. 3 shows the change in the 1-sigma jitter error $(\sigma_{tDLL})_m$ in m unit according to the change in $(C/N_0)_{dBHz}$ when $B_n$ = 0.2 Hz, $T$ = 0.02 sec, $D$ = 1 chip, and $b$ =2. The figure verifies that the jitter error rapidly increases as $(C/N_0)_{dBHz}$ decreases.

$$(\sigma_{tDLL})_m = (\sigma_{tDLL})_{chip} \cdot \left(\frac{c}{R_c}\right)_{m/chip} \quad (6)$$

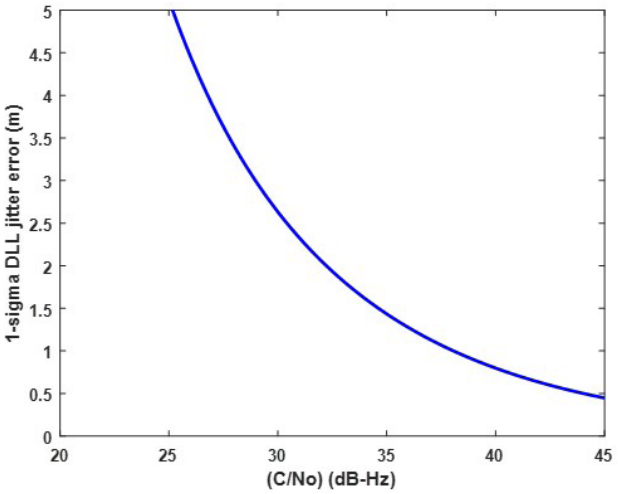


**Fig. 3.** Calculated 1-sigma error of DLL jitter by C/N0 variation.

In summary, ranging measurement errors of a receiver affected by a jammer can be modeled by Eqs. (1-6) that describes the DLL error considering the jamming to noise ratio, the antenna gain towards the satellite, the antenna gain towards the jammer, and the carrier-to-noise ratio.

## 3. INDIRECT VERIFICATION OF DESIGNED MODEL

Although actual verification of the ranging measurement error model is highly desirable, it is difficult to transmit real jamming signals for experiment due to the strict national radio wave regulations. In addition, even if jamming signals are generated and applied using GPS simulators, it cannot be considered as an actual verification due to the use of simulated signals. Accordingly, this study performed a verification on the jammer's influence model on ranging measurements indirectly rather than directly through the user's receiver jamming influence tests, which were performed in the preceding studies. Glomsvoll (2014) installed a user receiver on the shore and mounted a jammer in a boat to perform a test of identifying the jamming influence on user receivers, moving the boat from 1,300 m away from the user receiver and approaching the shore slowly. The test overview performed by Glomsvoll is shown in Fig. 4, in which a user receiver is installed at location D, and a boat mounted with a jammer moves toward location D straightly from location B.

The analysis on jamming effect was based on the change in C/N0 measured at the receiver and the calculated horizontal and vertical errors. The jammer used by Glomsvoll

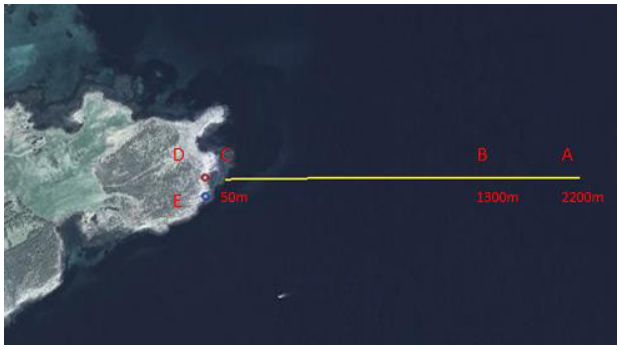


**Fig. 4.** Experiment overview (Glomsvoll 2014).

**Table 4.** Description of parameters used in the jamming simulation

| Parameter | Value | Parameter | Value |
|---|---|---|---|
| $f_1$ | 1575.42 MHz | $Q$ | 2.22 |
| $G_t$ | 3 dBic | $R_c$ | 1.023 Msps |
| $G_i$ | 6 dBic | $b$ | 2 Hz |
| $L_f$ | 3 dB | $D$ | 1 chip |
| $(C/N_0)_{eff\,dBHz}$ | 28 dBHz | $B_n$ | 0.2 Hz |
| $G_{svi}$ | 1.5 dBic | $T$ | 0.02 sec |

transmitted jamming signals at -35 dBW and 1575.42 MHz, which was a frequency band of GPS L1 C/A. Since other jammer-related variables were not disclosed, the same variables that were used to depict Figs. 1-3 were used. Table 4 summarizes the variables used in this indirect verification. Fig. 5 shows the comparison between C/N0 measured when a jammer approached the user receiver for about three min from 1,300 m away and C/N0 calculated from the model formulated in this study. The left side of Fig. 5 shows C/N0 measured in the test and the right side shows C/N0 calculated by the designed model. Fig. 5 verifies that there is similarity between measured and calculated C/N0 values.

Glomsvoll verified the horizontal and vertical ranging errors of the user receiver while measuring C/N0 at the same time. This study calculated the level of ranging measurement errors using the actually measured C/N0 at the receiver to compare the ranging errors indirectly. The left side of Fig. 6 shows the measured C/N0 value, but the fluctuation of the values is so large that the measured C/N0 value is curve-fitted as shown in the right side of Fig. 6. Signals whose C/N0 is approximately below 30 dBHz could no longer be traced in the receiver.

The DLL errors of eight pseudorandom noise (PRN) were calculated from the curve-fitting C/N0 values, respectively. Glomsvoll did not provide the pseudorange, user position, and satellite positions in detail. Thus, the pseudorange and satellite positions were calculated arbitrarily based on the measured C/N0 to calculate the ranging error, which are presented in Table 5. After applying the DLL delay error to the pseudorange for each PRN, the horizontal and vertical

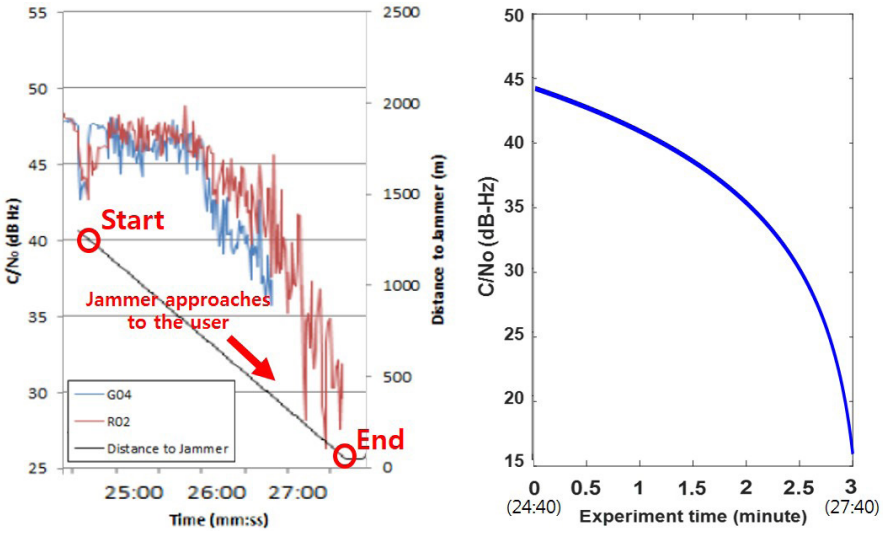


**Fig. 5.** Comparison of between the measured C/N0 (left; Glomsvoll 2014) and the calculated C/N0 by designed model (right).

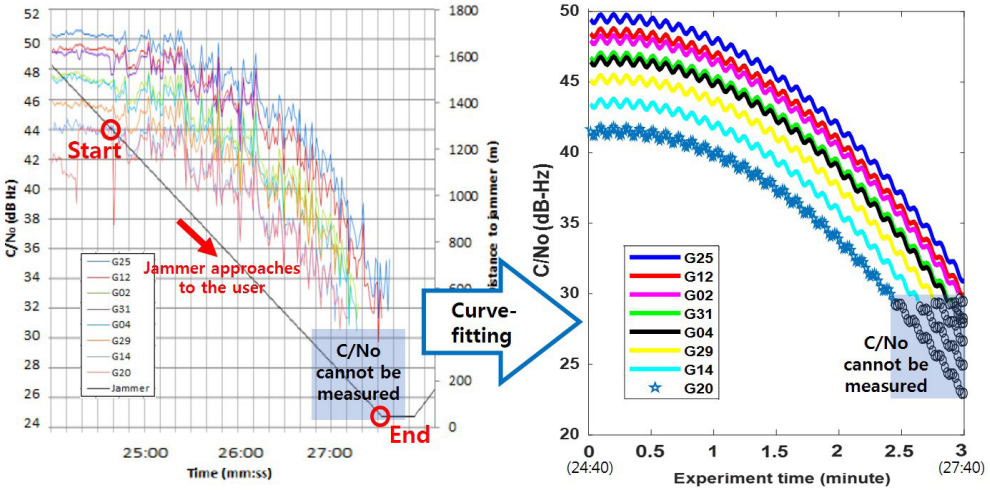


**Fig. 6.** Measured C/N0 (left; Glomsvoll 2014) and the curve-fitted measured C/N0 (right).

**Table 5.** Description of the assumed positions and the pseudoranges by C/N0.

| SV / User | PRN | C/N0 (dBHz) | Position (LLH) | | | Pseudorange (m) |
|---|---|---|---|---|---|---|
| | | | Latitude (deg) | Longitude (deg) | Height (km) | |
| GPS 1 | 25 | 49.45 | 40 | 150 | 19500 | 19916699.71 |
| GPS 2 | 12 | 48.45 | 70 | 140 | 20000 | 21324350.83 |
| GPS 3 | 31 | 47.95 | 50 | 120 | 21000 | 21222720.13 |
| GPS 4 | 2 | 46.75 | 30 | 80 | 20500 | 22310577.29 |
| GPS 5 | 4 | 46.45 | 10 | 100 | 21000 | 22582236.98 |
| GPS 6 | 29 | 45.15 | 0 | 170 | 20000 | 23272061.23 |
| GPS 7 | 14 | 43.45 | 25 | 140 | 24000 | 24342834.71 |
| GPS 8 | 20 | 36.45 | 20 | 40 | 20000 | 25550143.31 |
| User | - | - | 37.5975 | 126.8651 | 0.063576 | - |

errors were calculated. Figs. 7 and 8 show the comparisons of horizontal and vertical errors. The left sides of Figs. 7 and 8 show the horizontal and vertical errors calculated at the receiver. The right sides of Figs. 7 and 8 show the horizontal and vertical errors generated by the DLL error modeling through the curve-fitting C/N0. Both Figs. 7 and 8 showed that the errors occurred in the actual jamming situation were somewhat larger than the calculated ranging errors by C/N0, but it was verified that the overall error trends of both methods were similar.

## 4. CONCLUSIONS

This study proposed an effective error model of ranging measurements of navigation receivers due to jamming. The measurement error modeling was performed based on jammer and receiver-related variables and the rationale

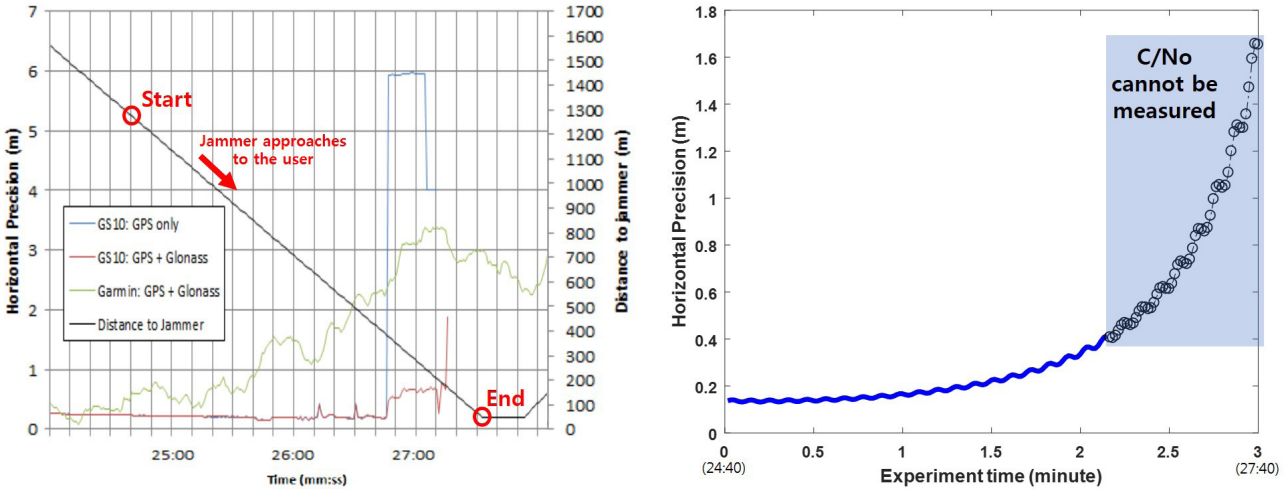


**Fig. 7.** Comparison of horizontal precision with the actual jamming environment (left; Glomsvoll 2014) and ranging measurement error model (right).

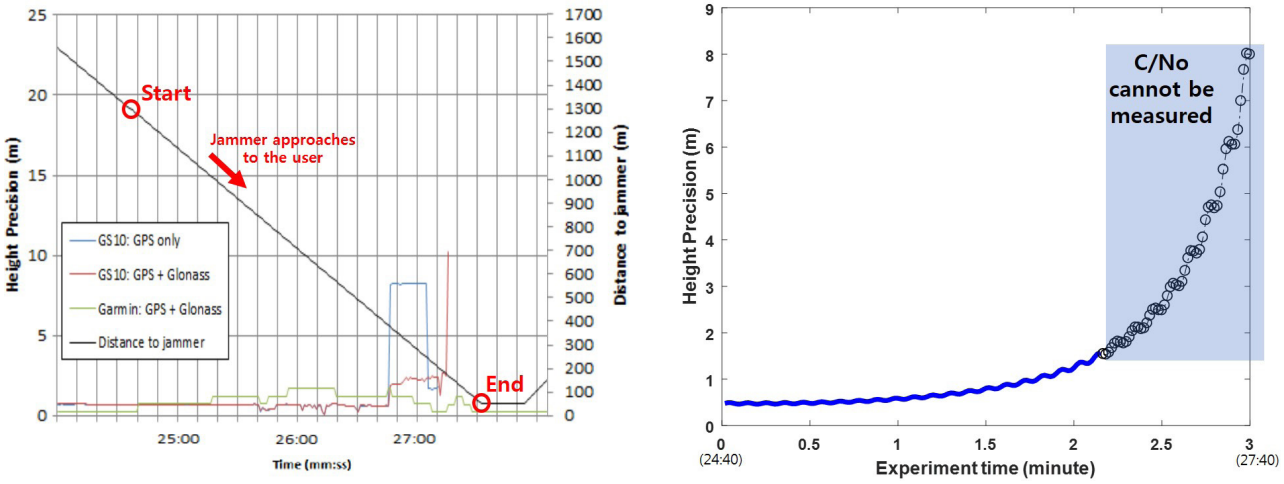


**Fig. 8.** Comparison of height precision with the actual jamming environment (left; Glomsvoll 2014) and ranging measurement error model (right).

that DLL errors may occur in the receiver if the difference between the jamming signal power and the navigation signal power is not large. Although the navigation error occurred in the actual jamming situation were somewhat larger than the ranging errors calculated by the proposed method, it was verified that the overall error trends of the reported actual jamming experiment results and the proposed model showed good consistency.

## ACKNOWLEDGMENTS

This work was supported by the National GNSS Research Center of Defense Acquisition Program Administration and Agency for Defense Development. The first author was supported by Expert Education Program of Maritime Transportation Technology (GNSS Area), Ministry of Oceans and Fisheries of Korean government.

## AUTHOR CONTRIBUTIONS

Conceptualization, W. J. Yoo; Methodology, W. J. Yoo, H. Kim, D. H. Hwang, H. So; Software, W. J. Yoo, H. Kim, D. H. Hwang, H. So, and H. K. Lee; Writing, W. J. Yoo; Review and editing, H. K. Lee.

## CONFLICTS OF INTEREST

The authors declare no conflict of interest.

## REFERENCES

Choi, C.-M. & Ko, K.-S. 2015, A Study on Development Direction of Navigation System for NAVWAR, Journal of the Korea Institute of Information and Communication

Engineering, 19, 756-763. https://doi.org/10.6109/jkiice.2015.19.3.756

De Lorenzo, D. S., Rife, J., Enge, P., & Akos, D. M. 2006, Navigation accuracy and interference rejection for an adaptive GPS antenna array, in Proc. ION GNSS, 2006, pp.763-773

Fu, L. & Zhu, Y. 2011, A study on GPS integrity monitoring algorithms based on ultra-tight integration system. In Industrial Electronics and Applications (ICIEA), 6th IEEE Conference on, 21-23 June 2011, Beijing, China, pp.596-600. https://doi.org/10.1109/iciea.2011.5975655

Glomsvoll, Ø. 2014, Jamming of GPS & GLONASS signals-a study of GPS performance in maritime environments under jamming conditions, and benefits of applying GLONASS in Northern areas under such conditions, Master thesis, The University of Nottingham. http://hdl.handle.net/11250/2389675

Grant, A., Williams, P., Ward, N., & Basker, S. 2009, GPS jamming and the impact on maritime navigation, Journal of Navigation, 62, 173-187. https://doi.org/10.1017/s0373463308005213

Kaplan, E. & Hegarty, C. 2005, Understanding GPS: principles and applications, 2nd ed. (Norwood: Artech house)

Kim, K.-Y. 2013, Analysis of anti-jamming techniques for satellite navigation systems, The Journal of Korea Institute of Communications and Information Sciences, 38, 1216-1227. https://doi.org/10.7840/kics.2013.38c.12.1216

**Won Jae Yoo** received the B.S. and M.S. degree in School of Electronics and Information Engineering, Korea Aerospace University in 2014 and 2016 respectively. He is a doctorial course student at Navigation and Information Systems Laboratory (NISL), Korea Aerospace University. His research interests include Assisted GNSS, software GNSS receiver, Software Defined Radio and its applications.

**Heyone Kim** received B.S. degree in the Department of Electronics Engineering, Chungnam National University, in 2017. His research interests include gyro-free inertial navigation system and modeling & simulation software.

**Dong-Hwan Hwang** is a professor in the Department of Electronics Engineering, Chungnam National University, Korea. He received his B.S. degree from Seoul National University, Korea in 1985. He received M.S. and Ph.D. degree from Korea Advanced Institute of Science and Technology, Korea in 1987 and 1991, respectively. His research interests include GNSS/INS integrated navigation system design and GNSS applications.

**Hyoungmin So** is a senior researcher of Agency for Defense Development (ADD) in Korea, Republic of. He received the B.S. degree in mechanical engineering at Korea University. He received the M.S. and Ph.D. degree in aerospace engineering at Seoul National University (SNU). He worked in the field of GNSS and pseudolite receiver development including SDR and vector tracking loop algorithm in SNU GNSS laboratory. Since 2011, he's been working for ADD. His research interests are GNSS receiver, anti-jamming/spoofing algorithm, and WADGPS technologies.

**Hyung Keun Lee** received the B.S. and M.S. degrees in control and instrumentation engineering and the Ph.D. degree from the School of Electrical Engineering and Computer Science from Seoul National University, Republic of Korea, in 1990, 1994 and 2002, respectively. From 1994 to 1998, he was with Hyundai Space and Aircraft Corporation, Republic of Korea. Since 2003, he has been with the School of Electronics and Information Engineering at Korea Aerospace University, Republic of Korea, as a professor. His research interests include positioning and navigation systems.